

Characteristics of Annular Mixing Layer in High Subsonic Jet

Murugan, K.N.^a and Sharma, S.D.^a

Department of Aerospace Engineering, Indian Institute of Technology Bombay,
Powai, Mumbai -400076. knmurugan@aero.iitb.ac.in (Murugan K N)
sds@aero.iitb.ac.in (Sharma S D)

Abstract

Experimental studies were conducted on an annular mixing layer which evolved from freely expanding adiabatic circular jet produced by a conical nozzle. The mixing layer region shrouding the potential core was explored at four different jet-exit Mach numbers - 0.5, 0.6, 0.7 and 0.8. Pressure measurements were carried out by means of a miniature Pitot probe attached to an automated traverse. Mean velocity profiles were obtained from the radial distribution of pressures across the annular mixing layer thickness at various axial locations. The iso-velocity curves, plotted in longitudinal plane, exhibited that the velocity in the line of the nozzle lip was always about 60% of the nozzle exit velocity for the entire range of Mach numbers studied. The mixing layer thickness, assessed in terms of vorticity thickness, was found to grow linearly with the longitudinal distance downstream of the nozzle. The mixing layer growth rate was found to decline with increasing Mach number. However, the mixing layer was found to possess a strong self-similarity with a unique profile common to all the Mach numbers. The entrainment of mass into the mixing layer was found to increase along the streamwise distance at a constant rate depending on the nozzle-exit Mach number – increase in the Mach number resulting in decrease in the entrainment. The present work also suggests that nozzle with higher convergence angle tends to enhance the spread of the mixing layer along with the entrained mass.

NOMENCLATURE

D - nozzle exit diameter

m - mass flow rate

m_e - mass flow rate at the nozzle exit

M - Mach number (u/a)

p - Pitot pressure

p_a - ambient pressure

r - radial distance from the jet axis

$R_{0.5}$ - radial distance from the jet axis to a location where velocity u is half of U_e

u - axial velocity

U_e - centerline velocity at the nozzle exit

x - axial distance from the nozzle exit

1. INTRODUCTION

A mixing layer is the region between two co-flowing streams moving at different velocities. An annular mixing layer is formed either around a round jet or between two co-axial jets. Flow visualization studies using color dye by Winant and Brown [1] showed for the first time the vortex formation in a plane mixing layer. It was reported that the vortex pairing and its associated dynamics is responsible for mass entrainment, spread rate and primary mechanism of noise generation. The detailed experimental study was carried out by Brown and Roshko [2] to examine the effect of velocity ratio, density ratio and compressibility on mixing layer growth and mass entrainment. The velocity ratio and compressibility were found to have strong influence on mixing layer growth and mass entrainment compared to density ratio. Moreover, to quantify the mixing layer thickness, a term vorticity thickness

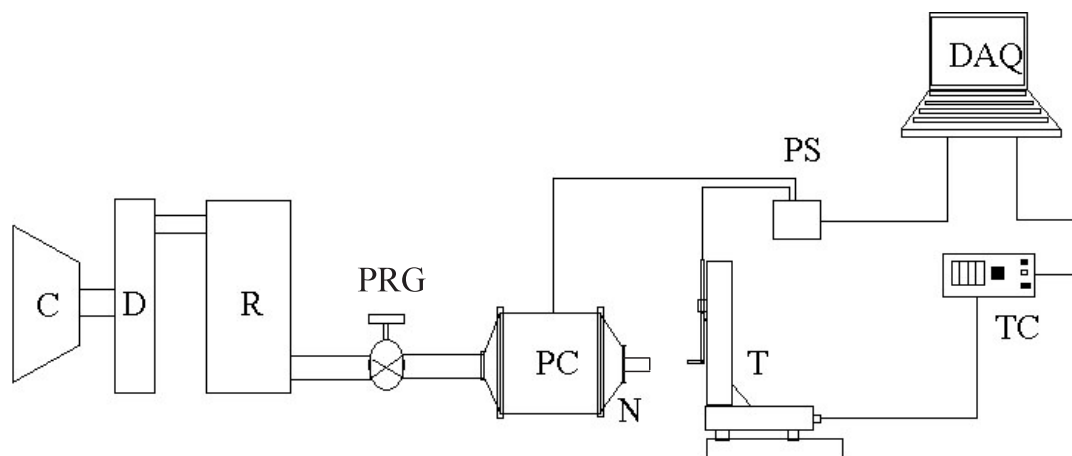
was introduced and detailed methodology for obtaining vorticity thickness was discussed.

Crow and Champagne [3] reported the existence of large scale flow structures in mixing layer region of jet flow. The rate of mass entrainment along the jet stream was reported to approach a constant value of 0.13 ± 0.01 in the initial region of a low speed jet. Maestrello and McDaid [4] experimentally found that in a freely expanding jet, different streamwise regions had different self-similarity and different rates of spread and mass entrainment. Hussain and Zedan [6] exclusively reviewed the effect of initial conditions on axisymmetric free shear layer and reported that the self-preservation state of mixing layer depends on the momentum thickness at the nozzle exit. Lau et al. [7] used laser velocimeter in the mixing layer of iso-thermal jet flows with Mach number of 0.28, 0.90 and 1.37, and found that the Mach number plays a determining role in the development of a mixing layer. They emphasized that the results could be significantly affected by the measurement techniques employed. Freund et al. [8] used Direct Numerical Simulation to investigate the effect of compressibility in turbulent annular mixing layer by considering the nine cases of convective Mach numbers ranging from 0.1 to 1.8 and found that turbulence Mach number can reach as high as 0.8. It was further reported that the large scale azimuthally correlated rollers dominated the low Mach number region of mixing layer whereas streamwise oriented structures dominated the flow in high Mach number region.

It is evident from various investigations that the annular mixing layer is dominated by large scale coherent structures wherein the initial conditions can play important role. The increase in compressibility suppresses the growth of mixing layers. The present work aims to establish the relation between jet Mach number and mixing layer growth through simple measurements. In addition, the effect of nozzle convergence angle on mixing layer is also studied

2. EXPERIMENTAL METHOD

Figure 1 shows the schematic diagram of the test setup used for the present study. A high pressure reservoir with 30 m^3 capacity is charged with dry air by means of a two-stage reciprocating compressor which is driven by a 90 hp electric motor. The compressor delivers 5.7 m^3 of air per minute at a pressure of 14 kg/cm^2 which is adequate for a 50 mm diameter nozzle running continuously at choked condition. A globe valve is manually operated to regulate the constant mass flow rate in order to maintain the desired pressure in a cylindrical plenum chamber which is 332 mm in diameter and 550 mm long. A steel pipe of 36 mm internal diameter with smooth finish connects the test nozzle to the plenum chamber. The test nozzle is machined out of brass with 150 mm length and 20 mm exit diameter with lip thickness of about 1 mm resulting in a half convergence angle of about 3 degree.



C- Compressor, D –Dryer, R-Reservoir, PRG- Pressure Regulating Valve, PC- Plenum Chamber, N- Nozzle attach
T- Traverse with pitot-tube, TC- Traverse Controller, PS – Pressure Scanner, DAQ- Data Acquisition system.

Figure 1. Schematic diagram of the test facility

A miniature Pitot probe was made out of stainless steel hypodermic tube with outer diameter of 0.7 mm. The mouth of the Pitot probe was chamfered using 0.6 mm drill-bit to minimize the flow spillage around the free tip and also to make the probe less sensitive to the flow angle. A larger diameter stem was provided in telescopic fashion so as to provide rigidity to stand the impact of the high speed jet. The Pitot probe was mounted on a two-dimensional computerized automatic traverse. It can traverse upto 610 mm in two orthogonal directions in the minimum step size of 0.25 mm at a speed of 25 m/s. With reference to the ambient atmospheric pressure, using isentropic flow relations, the plenum chamber pressure was calculated for a predetermined Mach number of the flow at the nozzle exit plane and was maintained by means of pressure regulating valve. Pressures were registered by Pressure Systems make transducers, PSI model 9116 with 16 channels. The pressure transducer is capable of measuring 103 kPa gauge pressure with an accuracy of $\pm 0.05\%$ of full scale and measurement resolution of $\pm 0.003\%$ full scale. It uses NUSS software for acquiring the data at a scanning rate of 500 samples per second.

Experiments were conducted in adiabatic jets at the plenum chamber temperature of about 300 ± 2 K. The Reynolds number varied in a range of 1.63 to 2.72×10^5 based on the nozzle exit diameter and velocity. Pitot-pressures were measured in a step of 0.5 mm in radial direction at ten different axial locations downstream of the nozzle. For the jet flow produced in open atmosphere, the ambient pressure is considered as the static pressure and the settling chamber temperature (which is nearly the same as the ambient temperature) is considered as the stagnation temperature. Assuming the flow to be isentropic, the Mach number and the velocity in the jet were calculated from the pressure and temperature ratios. The volume of the settling chamber is only 0.16 % of that of the high pressure reservoir. Further, the maximum settling chamber pressure is about 5 % of the reservoir pressure (the reservoir is fed continuously by the compressor). Thus, even with the jet on, the pressure difference between the reservoir and the settling chamber remains almost constant. This enabled the manual control considerably easy as it was required to be employed very slowly. The average chamber pressure maintained over the entire period of the test is reported in Table 1. The small deviation reflects that manual control employed in maintaining the settling chamber pressure is adequately accurate.

Table 1. Control of settling chamber pressure

S. NO	Test Mach	Calculated Chamber Pressure (psi)	Measured Chamber Pressure (psi)	Deviation
1	0.8	7.594	7.620	$\pm 0.29\%$
2	0.7	5.596	5.610	$\pm 0.320\%$
3	0.6	3.989	4.009	$\pm 0.542\%$
4	0.5	2.691	2.701	$\pm 0.674\%$

2.1 Uncertainty Analysis

Uncertainty analysis has been performed for the instrumentation involved in the pressure measurements such as pressure transducer, barometric pressure transducer and thermometer. Pressure transducer has the uncertainty value of ± 3.0 Pa and Barometric transducer has an uncertainty of ± 0.5 Pa, and thermometer ± 0.5 deg C. The combined uncertainty in estimating the velocity is too small and it is shown in the Table 2.

Table 2. Estimated Uncertainties in Measurement

Intended test Mach number	Measured Mach number along the jet centerline	Velocity along the jet centerline (m/s)
0.5	$0.499159 \pm 2.0 \times 10^{-5}$	168.966 ± 0.071
0.6	$0.598984 \pm 1.6 \times 10^{-5}$	201.608 ± 0.084
0.7	$0.698733 \pm 1.3 \times 10^{-5}$	231.101 ± 0.096
0.8	$0.800156 \pm 1.0 \times 10^{-5}$	261.28 ± 0.11

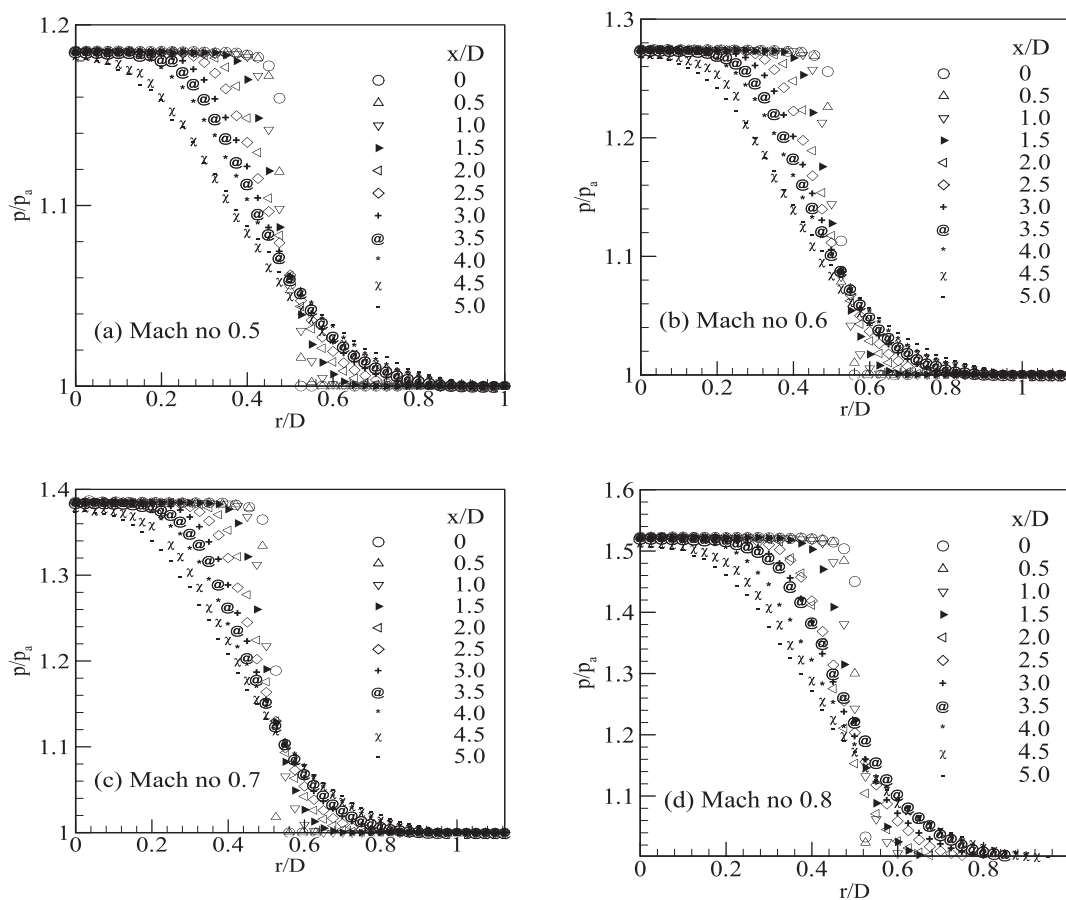


Figure 2. Radial pressure distributions at several axial locations

3. RESULTS AND DISCUSSION

Pressure profiles obtained for different nozzle exit Mach numbers of 0.5, 0.6, 0.7 and 0.8 at several axial locations are shown in Figure 2. The pressure along the centerline remains constant from the nozzle exit up to $5D$. This is the potential core region wherein annular mixing layer evolves around the jet. Further, it is to be noted for all the nozzle-exit Mach numbers that the pressure profiles seem to intersect at around $r/D = 0.5$ which is the nozzle lip line.

Figure 3 shows plots of iso-velocity lines, obtained from data presented in Figure 2, in $x-r$ plane. These lines are nearly straight and the one along the nozzle lip line having zero slope is the locus of the

velocity which is about 60% of the jet exit velocity at all the Mach numbers. The region demarcated by the iso-velocity lines of 10% and 90% of the nozzle exit velocity is indicative of the mixing layer spread [7] which appears to shrink as the jet Mach number is increased. For example, the spread angle estimated from these plots is found to decrease from approximately 8.6 degree to 7.7 degree when the nozzle exit Mach number is increased from 0.5 to 0.8. This observation explains as to why the length of potential core of a jet increases with the jet Mach number.

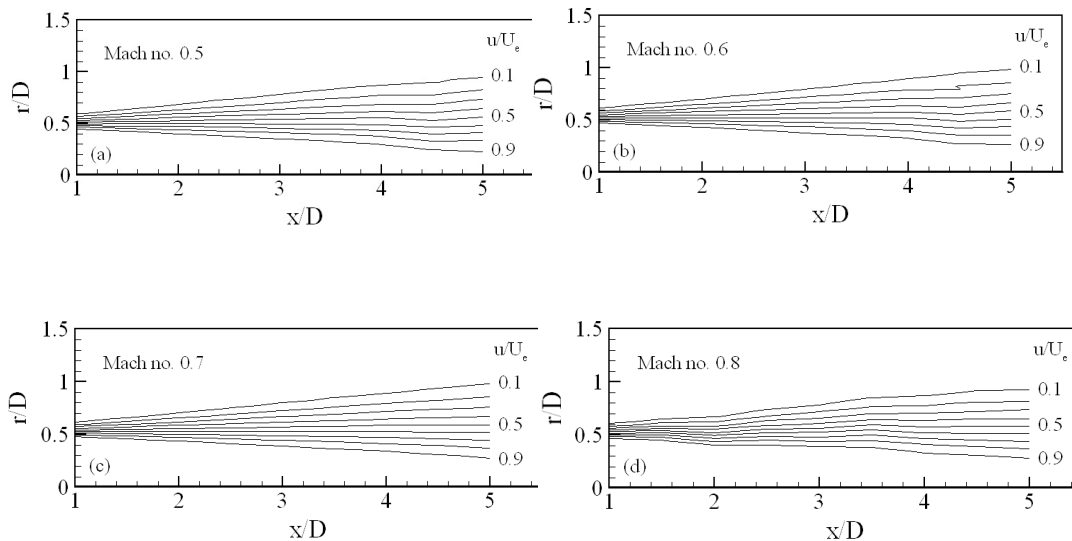


Figure 3. Iso-velocity lines in longitudinal plane

It is well documented that the mixing layer evolves self-similarity with linearly growing thickness [11]. In order to test self-similarity in mixing layer, the normalized velocity obtained from Figure 2 is plotted as function of similarity parameter $\eta = (r-R_{0.5})/x$ and shown in Figure 4. For each of the Mach number, the data exhibit a remarkably good collapse on to a single curve confirming the existence of self-similarity in the mixing layer region.

All the profiles from Figure 4 (a) to (d) for the four different Mach numbers were collected and plotted together. That composite plot is shown here in Figure 5. Again, the collapse of the data in the entire region, except in the initial region very close to the jet periphery, is incredible. On the basis of the observation of Figure 5, it can be said that for a given test setup, the mixing layer possess a strong self-similarity which is independent of the jet Mach number.

Following Brown and Roshko [2], the maximum velocity gradient, $(\partial u/\partial r)_{\max}$, obtained from the velocity profiles at each longitudinal locations, was used to calculate the vorticity thickness, $\delta = U_e/(\partial u/\partial r)_{\max}$, which is representative of the mixing layer thickness. The mixing layer thickness thus determined is plotted against the axial distance in Figure 6 for various jet Mach numbers. It is evident that the annular mixing layer grows linearly along the longitudinal distance. Further, the plot clearly shows that increasing flow compressibility restricts the physical thickness of the mixing layer. The slope of these curves would give growth rate of mixing layer at different jet Mach number.

Figure 7 shows the dependency of the growth rate of the mixing layer (obtained from the slope of curves shown in Figure 6) on the jet Mach number. Experimental data acquired using different measurement techniques by various researchers are also included for comparison. For example, Lau et al.[7] used laser velocimeter, Carey used interferometer [in 7], Arakeri et al. used PIV [10], Birch and Eggers [5], Brown and Roshko [2], and Sharma and Madan [10] used pitot tube. All the data, except those due to Birch and Eggers [5], follow a definite smooth trend represented by

$$\delta^* = 0.167 - 0.046 M^2$$

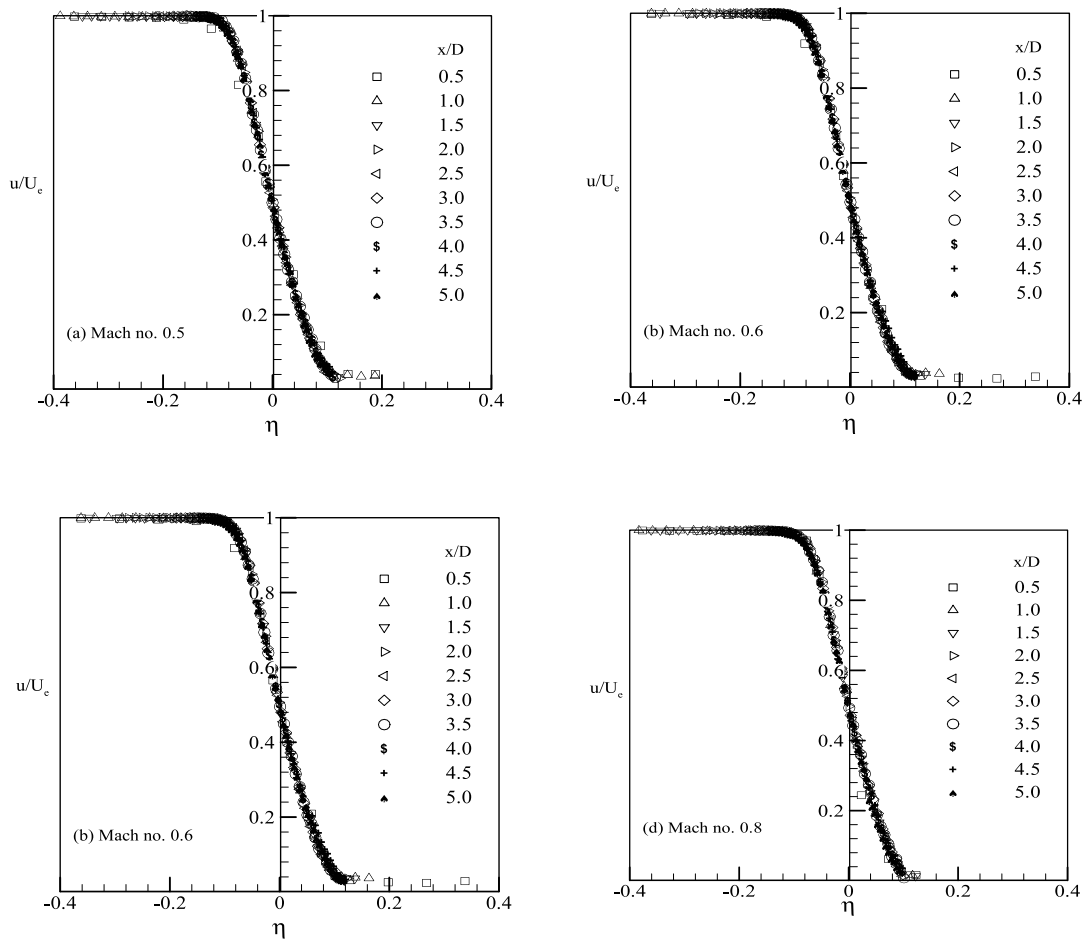


Figure 4. Normalized velocity profiles in mixing layer

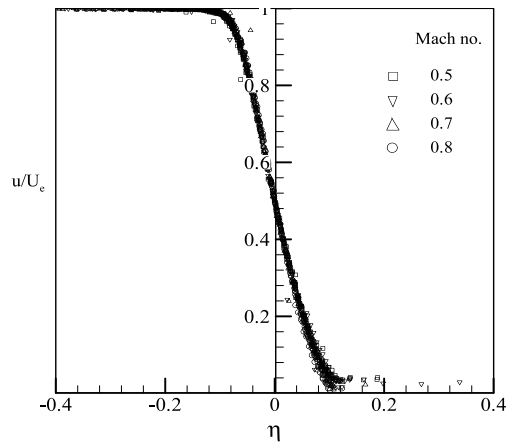


Figure 5. Influence of March number normalized velocity

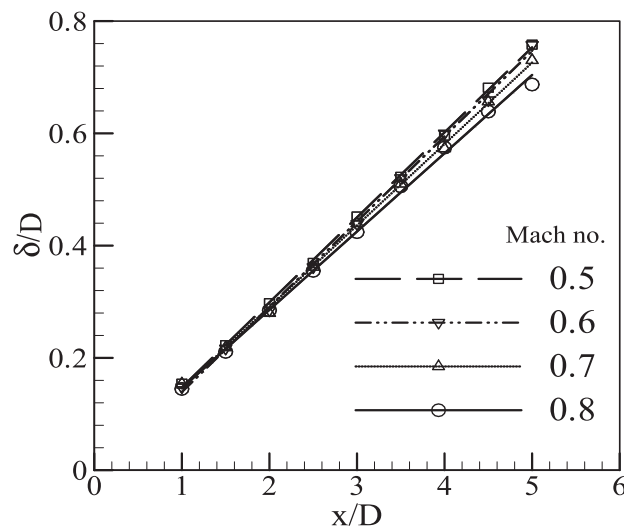


Figure 6. Axial variation of Vorticity thickness in annular mixing layer region

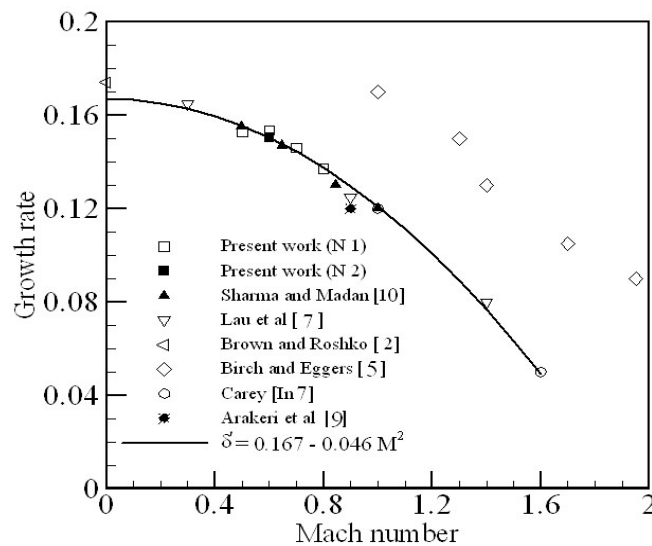


Figure 7. Effect of Mach number in Mixing Layer growth rate

A significant departure of the data of Birch and Eggers is said to be due to the effect of physical presence of the Pitot tube in the flow [7]. In the present case, a miniature probe with only 0.7 mm diameter was used whose open end was chamfered. The small size of the measuring probe compared to the physical thickness of mixing layer and its large internal diameter to external diameter ratio at the tip helped in minimizing the streamline displacement effect due to the presence of the probe in the mixing layer. As a result, the data obtained were more or less free from interference effect and matched with the data obtained by other researcher who used advance techniques like PIV, LDV and hotwire. However, a common trend that is reflected is that the growth rate of a mixing layer diminishes with an increase in the nozzle exit Mach number. Extension of the curve suggests that for an extreme case of $M = 0$ (incompressible jet flow) the mixing layer spread rate would approach 0.167 which is quite close to 0.174, a value reported by Brown and Roshko [2] for incompressible mixing layer. Whereas the curve towards higher Mach number seems to suggest that the mixing layer would virtually cease to grow when the nozzle exit Mach number is increased to about 1.9. But such surmise is physically not valid as the growth rate of the mixing layer at such high Mach numbers varies inversely with the nozzle Mach number [2]. Moreover, what emerges from the careful observation of the data collated in Figure 7 is that the growth characteristics of two mixing layers formed by isothermal jets [7] and the present

adiabatic jets are identical, irrespective of their different thermodynamic states. This fact, however, remains to be verified for high temperature jets with combustion.

The mass entrainment from the surrounding into the jet flow was calculated from the measured data at each axial location using the following expression.

$$m(x, r) = 2\pi \int_0^{R(x)} \rho(x, r) u(x, r) r dr$$

Here, $R(x)$ is the maximum radial distance from the centerline, where the Pitot pressure approached the atmospheric pressure value. The entrained mass was found to increase more or less linearly with the axial distance. The non-dimensional entrainment rate $\left(\frac{d(m / m_e)}{d(x / D)} \right)$ was found to be 0.122, 0.121, 0.12, and 0.104 for the jet Mach numbers of 0.5, 0.6, 0.7, and 0.8, respectively. These values compare well with 0.13 ± 0.01 reported by Crow and Champagne [3] for incompressible flow and more recently by Arakeri et al. [9] for high subsonic jet flow ($M = 0.9$).

3.1 Effect of Nozzle Convergence angle

An attempt was also made to examine the effect of the convergence angle of the nozzle on the mixing layer growth pattern. A nozzle was constructed with the half convergence angle of 7 degree. The increase in the convergence angle is significant compared to the previous nozzle with 3 degree. The experiments were repeated for the nozzle exit Mach number of 0.6. Figure 7 shows comparison of results from both the nozzles – N1 with 3 degree and N2 with 7 degree half convergence angles.

It is surprising to note that there is hardly any discernible effect on the pressure profiles despite the significant difference in the convergence angles. However, the nozzle with increased convergence angle, which is expected to produce narrower Vena-contraction, produces a jet wherein the mixing layer exhibits more spread and higher entrainment rate.

CONCLUSIONS

The following conclusions are drawn from the present study.

1. The annular mixing layer grows linearly like a plane mixing layer.
2. The growth of a mixing layer is independent of the thermodynamic state of jet. However, it strongly depends on the compressibility of the flow.
3. In the range of jet Mach numbers of present investigation, the mixing layer possesses a strong self-similarity which is found to be independent of the Mach number.
4. Regardless of the jet Mach numbers, the velocity within the mixing layer along the lip line is found to be about 60% of the nozzle exit velocity.
5. The growth of the mixing layer is suppressed by increase in the jet Mach number and the spread rate is found to decline with square of the jet Mach number.
6. The non-dimensional entrainment rate is found to be 0.12 for all the Mach numbers in the present study

The increase in convergence angle of nozzle results in increase in mass entrainment which enhances the growth of the mixing layer

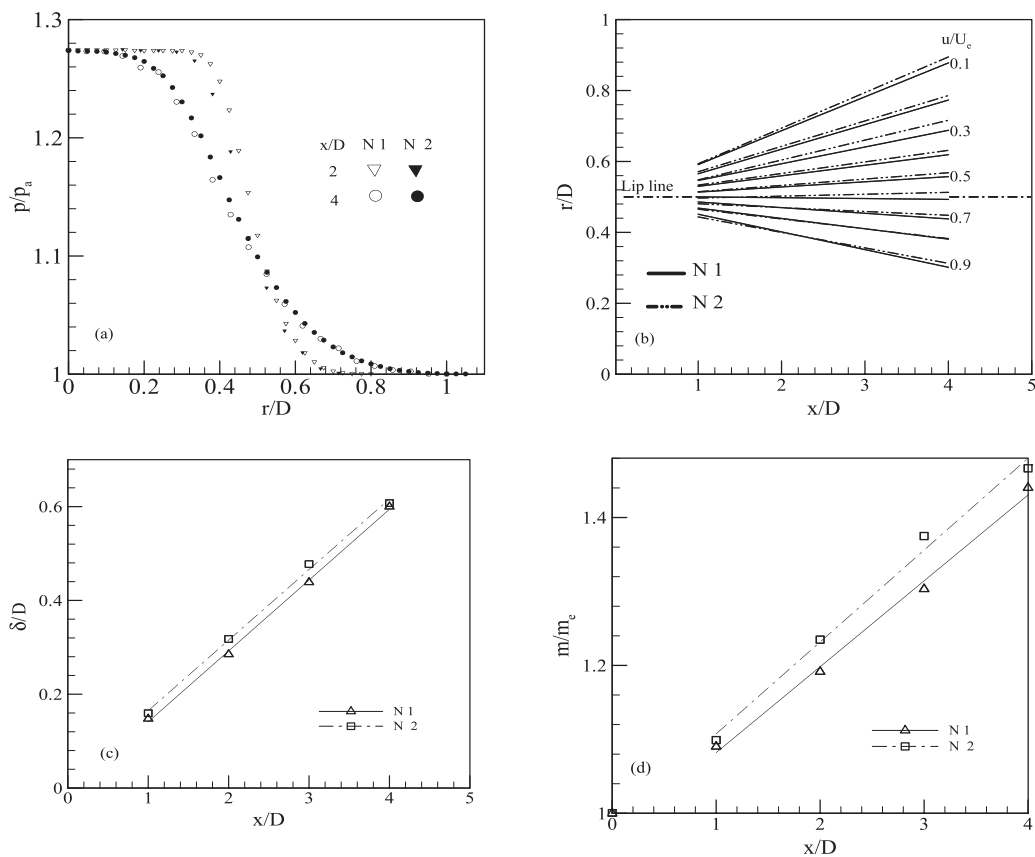


Figure 8. Mixing layer parameters for different convergence angles at Mach 0.6: (a) Radial Pressure distribution, (b) Iso-velocity lines, (c) vorticity thickness, and (d) mass entrainment

REFERENCES

- [1] Winant, C. D and Brown, F.K. Vortex pairing: the mechanism of turbulent mixing layer growth at moderate Reynolds numbers. *J. Fluid Mechanics*, 63, part 2, 1974, 237-255.
- [2] Brown, G L and Roshko, A. On density effects and large structure in turbulent mixing layers, *J. Fluid Mechanics*, 64 (4). 1974, 775-816.
- [3] Crow S.C. & Champagne, S. H. Orderly structure in jet turbulence. *J Fluid Mech.* 48, 1971, 547-591.
- [4] Maestrello and McDaid, E. Acoustic characteristics of a high-subsonic jet. *AIAA J.* 9(6), 1971, 1058-1065.
- [5] Birch, S. F. & Eggers, J. M. A critical review of the experimental data for developed free turbulent shear layers. NASA SP-321, Vol.1, 1972 , pp 11-40.
- [6] Hussian A. K and Zedan, M F. Effect of the initial condition on the axisymmetric free shear layer: Effects of initial momentum thickness. *Phys. Fluids* 21, 1978 , 1110-1112.
- [7] Lau J C., Morris, P. J and Fisher M J. Measurement in subsonic and supersonic free jet using a laser velocimeter. *J Fluid Mech.* 93, 1979, 1-27.
- [8] Freund, J. B, Lele S K and Moin P Compressibility effect in a turbulent annular mixing layer. Part 1 Turbulence and growth rate., *J. Fluid Mech.* 421, 2000, 229-267.
- [9] Arakeri V H., Krothapalli, A., Siddavarm, V, Alkisar, M B. and Lorenzo, L M. 2003 on the use of microjets to suppress turbulence in a Mach 0.9 axisymmetric jet. *J fluid Mech.* 490, 75-98.
- [10] Sharma, S. D.and Madan, K. 2007 Growth of compressible axisymmetric mixing layer. *Fluid Mech. & Fluid Power conference*, India.
- [11] A.A Townsend, *Structure of Turbulent Shear Flow* (Cambridge University Press, Cambridge, England, 1976).

